Hydraulic and Civil Engineering Technology VIII
M. Yang et al. (Eds.)

doi:10.3233/ATDE230775

Anti-Corrosion Study of Corrosion Inhibitor and Sacrificial Anode on Coastal Reinforced Concrete Structures

Huazhi ZHENG [a,1], Wei LIU [b] and Hao YAN [c]
[a] *Shenzhen Huiyan Expressway Co., Ltd., Shenzhen 518081, China*
[b] *Guangdong Expressway Development Co., Ltd., Guangzhou 510199, China*
[c] *Southeast University, Nanjing 211189, China*

Abstract. In order to improve the durability of coastal reinforced concrete structures, the effects of the mixed rust inhibitors, migrated rust inhibitors, and zinc-based sacrificial anodes on the reinforcement corrosion behaviors were investigated by linear polarizations and electrochemical impedance spectroscopies. Their rust resistance efficiency was also compared by static weight-loss tests, which were under different chloride concentrations and pH values in simulated concrete pore solution. The test results indicate that the anti-rust performance of the migrated rust inhibitor is weaker than that of the mixed rust inhibitor with the same content (1%) and chloride concentration. The anti-rust effect of the zinc-based sacrificial anode is better than that of the rust inhibitor under a higher chloride concentration (0.85mol/L). Under the same test time (1d), anti-rust content (1%) and chloride concentration (0.6mol/L), the rust resistance properties of each reagent are as follows: (Neutral environment) Zinc-based sacrificial anode < Migrated rust inhibitor < Mixed rust inhibitor, (Alkaline environment) Migrated rust inhibitor < Zinc-based sacrificial anode < Mixed doped rust inhibitor.

Keywords. Mixed rust inhibitor, migrated rust inhibitor, zinc-based sacrificial anode, reinforcement corrosion resistance, chloride concentration, pH value

1. Introduction

The durability of concrete structures in coastal areas has a significant impact on the safety and economic benefits of civil engineering construction. Chloride salt erosion is the main factor leading to durability issues in concrete structures in this area [1-4]. Enhancing the resistance of coastal concrete structures to chloride salt erosion has garnered widespread attention from scholars, experts, and engineering professionals [5-7].

Currently, there are several corrosion protection measures for reinforced concrete structures, including concrete re-alkalization, corrosion inhibitors for reinforcing steel, cathodic protection using sacrificial anodes, and the use of corrosion-resistant steel bars. Among these, corrosion inhibitors for reinforcing steel [8] offer the advantages of convenient application, cost-effectiveness, and prolonged protection for reinforced

[1] Huazhi ZHENG, Corresponding Author, Shenzhen Huiyan Expressway Co., Ltd., China; Email:844108385@qq.com

concrete structures. Sacrificial anode methods [9,10], on the other hand, boast wide availability of materials, ease of processing, and high corrosion inhibition efficiency, making these two corrosion protection methods widely used in practical engineering projects.

Jin et al. [11], in comparison to an electrochemical chlorine removal group, conducted research on chloride ion distribution within concrete protective layers, changes in corrosion inhibitors using the automatic potential titration method and organic element analysis, and measured the total alkalinity of the protective layers. Yan et al. [12] used magnesium aluminum alloy sacrificial anodes to discuss their corrosion resistance to steel in simulated concrete pore fluids. Although the above scholars have conducted more research on steel bar rust inhibitors and anode sacrificial methods, there is a lack of evaluation regarding their corrosion protection effects under the combined influence of chloride salts and pH. Therefore, this study employs linear polarization, electrochemical impedance spectroscopy analysis, and static weight loss testing to investigate the influence of chloride ion concentration and pH values on the corrosion behavior of steel reinforcement under the protection of internally incorporated and migratory corrosion inhibitors, as well as zinc-based sacrificial anodes. This research aims to provide a theoretical basis and technical support for the durability design and maintenance of steel-reinforced concrete structures in coastal environments.

2. Test Program

2.1. Test Materials and Equipment

The HPB235 plain round steel bars are used in the tests with a diameter of 8 mm, its composition (mass fraction) is C 0.16%, Mn 0.44%, Si 0.27%, Cu 0.013%, S 0.018%, P 0.0049%, and the rest is iron. Amino carboxylic acid type powder is selected as an internal rust inhibitor with a dosage of 600 g/m^3; Migration type rust inhibitor amino carboxylic acid water agent, applied to the surface of concrete until natural air drying, with a dosage of 0.272 L/m^2; Zinc-based sacrificial anode (Z) contains 60 g of zinc alloy inside and of high alkaline mortar outside prism (25mm× 25mm ×125mm) with a potential of -1100mV. The concrete pore fluid is simulated using a saturated Ca $(OH)_2$ solution, and the chloride ion concentration and pH value in the simulated solution are adjusted by adding NaCl and $NaHCO_3$ solutions. The solute purity is selected to be AR grade. The other end of the zinc-based sacrificial anode is connected to a carbon steel electrode, with a working surface diameter and area of 1.12mm and 1cm^2, respectively. The device connection structure is shown in figure 1.

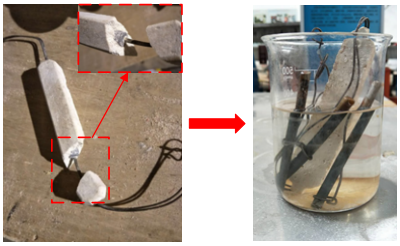

Figure 1. Connection and binding of zinc based sacrificial anodes.

The test is conducted in an experimental chamber (with a size of 800mm × 570mm ×505mm), and uses automatic sprinkler devices to simulate salt spray and rainwater areas in coastal environments. The PARSTAT4000 electrochemical workstation was selected for testing, with a carbon steel electrode, saturated calomel electrode, and platinum electrode used as the working electrode, reference electrode, and auxiliary electrode. The pH value in the solution was monitored using a Magneto PT-11 pH meter. The experimental setup is shown in Figure 2.

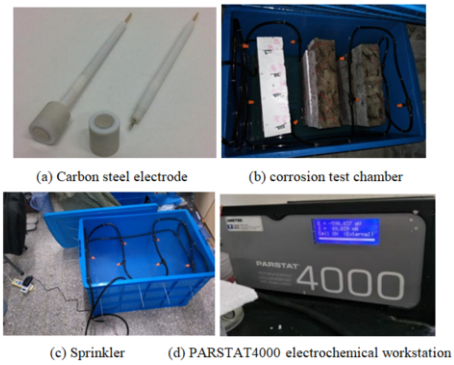

Figure 2. Testing equipment.

2.2. Design of the Test

A total of 5 test modes were adopted in the experiment (table 1), and electrochemical testing was conducted using the linear polarization method and AC impedance spectroscopy method. Each test mode used a carbon steel electrode, and the steel bar specimen was completely placed in the concrete simulated pore solution. Measurements were taken every 1 day for a total of 14 days. The electrochemical connection method in the experiment is presented in figure 3.

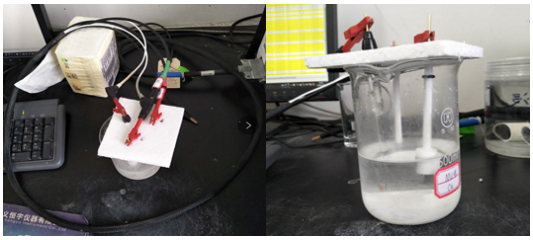

Figure 3. Test circuit connection for simulating concrete pore solution.

Table 1. Preparation of simulated concrete pore solution.

Test mode	NaCl concentration	pH value
C_0	0	12.5
C_1	0.6mol/L	12.5
C_2	0.85mol/L	12.5
C_3	0.6mol/L	8.5
C_4	0.6mol/L	10.0

The static experimental method in the test is as follows:

(1) Steel bars were cut into 100 mm long, using a polishing machine and 95% ethanol to remove stains and rust on the surface of the steel bars, then clean with acid and water, and finally blow dry.

(2) Numbered the steel bars and measure their corresponding initial mass (W_0), then place them in the simulated solution for the corresponding working conditions and measure them according to the test cycles of 7 days, 21 days, and 42 days.

(3) Take a steel rod at each experimental cycle, clean and dry it, and measure its final mass (W_1).

(4) The calculation of steel corrosion rate and protection efficiency for different test cycles is shown in equations (1) and (2):

$$v = \frac{W_0 - W_1}{ST} \tag{1}$$

$$IE_{\mathrm{w}} = \frac{v_0 - v_1}{v_0} \times 100\% \tag{2}$$

where, v is the corrosion rate of steel bar (mg/(cm^2·d)), v_0 and v_1 is the corrosion rate of steel bar without and with protection, respectively (mg/(cm^2·d)); S is the surface area of steel bar (cm^2); T is the time for steel bar weight loss experiment; IE_{W} is the protection efficiency.

3. Testing Results and Analysis

3.1. Analysis of Protective Effects under different Chloride Ion Concentrations

3.1.1. Linear Polarization Analysis

Figures 4 (a)~(c) and 5 (a)~(c) show the time-dependent curves for the corrosion potential and corrosion current density of the carbon steel electrode at different chloride ion concentrations. The experiment indicates that with increasing chloride ion concentration, the corrosion potential of the carbon steel electrode with both types of corrosion inhibitors and the reference blank group carbon steel electrode all decrease, while the corrosion current density increases. The extent of these changes, from largest to smallest, is as follows: blank group carbon steel electrode (EB electrode)>carbon steel electrode mixed with migration type rust inhibitor (E_0 electrode)>carbon steel electrode mixed with internal doping type rust inhibitor (E_6 electrode). These results suggest that whether or not rust inhibitors were added, carbon steel electrodes exhibited varying degrees of corrosion. Rust inhibitors all inhibited steel corrosion, and the rust inhibition effect of the internal type rust inhibitor was better than that of the migration type rust inhibitor. When the concentration of chloride ions increased from 0.6mol/L to 0.85mol/L, there was no significant change in the corrosion potential of E_B, E_0, and E_6 electrodes. However, the corrosion current density of E_B electrodes changed significantly, while the changes in E_0 and E_6 electrodes were very small. This indicates that carbon steel mixed with rust inhibitors can effectively suppress steel corrosion even in high-concentration chloride ion environments.

Combining Figures 4 (b) and 5 (b), the corrosion potential of the Z electrode decreased to -950mV after 3 days, indicating that the zinc-based sacrificial anode has a good protective effect on the corrosion of carbon steel electrodes. In addition, the

corrosion current density of the Z electrode increases with time, and the value is not only small but also has little change, indicating that the zinc-based sacrificial anode can also play a good and stable protective performance in high concentration chloride ion environments.

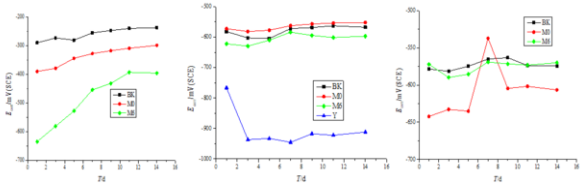

(a) C_0 (b) C_1 (c) C_2

Figure 4. Corrosion potential time-varying curve.

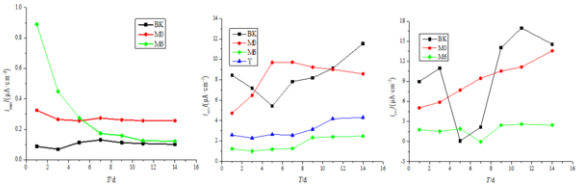

(a) C_0 (b) C_1 (c) C_2

Figure 5. Corrosion current density time-varying curve.

3.1.2. Electrochemical Impedance Spectroscopy Analysis

Figures 6 and 7 respectively provide the impedance spectra of carbon steel electrodes at different chloride ion concentrations. Figures 6 (a)~(c) present the Nyquist diagram of the electrode at 1d and figures 7 (a)~(c) show the Bode phase angle diagram of the electrode at 1d. The experimental results show that as the concentration of chloride ions increases, the electrode capacitance arc of carbon steel electrodes decreases, indicating that the polarization resistance decreases and the electrode corrosion resistance deteriorates. When the chloride ion concentration increased from 0.6mol/L to 0.85mol/L, there was no significant change in the capacitance arc of E_B and E_0 electrodes, indicating that the electrode impedance had reached saturation and the corrosion resistance had reached its limit at a chloride ion concentration of 0.6mol/L. From figures 6 (b) to (c), it can be seen that the capacitance arc of E_0, E_6, and Z electrodes is significantly larger than that of E_B electrodes, indicating that amino carboxylic acid type rust inhibitors and zinc-based sacrificial anodes have good rust resistance effects.

Figures 7 (b)~(c), indicate that both amino carboxylic acid type rust inhibitors can effectively inhibit corrosion rate and exhibit a “large impedance” phenomenon; the zinc-based sacrificial anode continuously outputs protective current to carbon steel, suppressing the anodic process on the surface of the protected steel rod and preventing corrosion of the steel rod. At the same time, it also accelerates the cathodic reduction reaction on the surface of the protected carbon steel. The accelerated reduction reaction consumes the electrons transported by the sacrificial anode, achieving a charge balance between the cathodic and anodic processes, enabling the cathodic protection process to continue. In addition, the phase angle of each electrode in the low-frequency region decreases with the increase of chloride ion concentration, indicating that electrode corrosion tends to be severe.

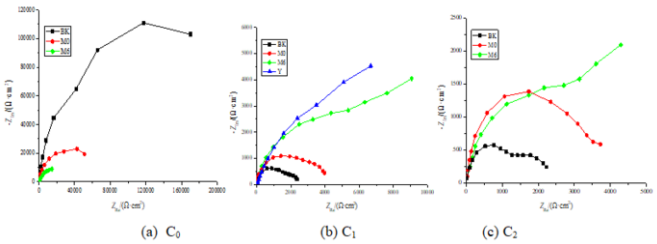

(a) C_0 (b) C_1 (c) C_2

Figure 6. Nyquist.

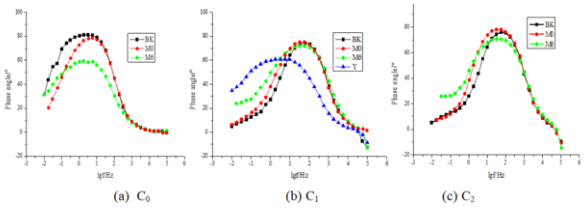

(a) C_0 (b) C_1 (c) C_2

Figure 7. Bode phase angle.

Fit the above impedance spectrum into an equivalent circuit and analyze the protective efficiency of carbon steel electrodes under various working conditions during 1-day testing. As shown in table 2, the corrosion inhibition efficiency of the migratory corrosion inhibitor slightly increases with higher chloride ion concentrations, while the corrosion inhibition efficiency of the internally incorporated corrosion inhibitor slightly decreases. This indicates that a chloride ion concentration of 0.6mol/L is the optimal protective environment for the internal doping type rust inhibitor (1% dosage); The optimal concentration of chloride ions in the migration type rust inhibitor (1% dosage) may exceed 0.85mol/L. Therefore, the rust resistance performance of the same amount of internal doping type rust inhibitor is better than that of the migration type rust inhibitor at the same chloride ion concentration.

Table 2. Protective efficiency of carbon steel electrodes under different chloride ion concentrations.

Cases	Solution electrical protection /($\Omega \cdot cm^2$)	Charge transfer prevention /($\Omega \cdot cm^2$)	Protection efficiency /%
C_0-E_B	73.42	239000	/
C_0-E_0	64.62	55140	/
C_0-E_6	56.2	24100	/
C_1-E_B	6.956	1369	/
C_1-E_0	7.499	3513	61.03
C_1-E_6	7.828	15280	91.04
C_1-Z	10.22	7625	82.05
C_2-E_B	4.821	1234	/
C_2-E_0	5.487	3526	65.00
C_2-E_6	5.397	9546	87.07

3.2. Analysis of Protective Effects under different pH Values

3.2.1. Linear Polarization Analysis

Figures 8 (a)~(c) and 9 (a)~(c) show the time-varying curves of corrosion potential and current density of carbon steel electrodes at different pH values. As the pH value decreases, the fluctuation of the time-varying curve of the EB electrode gradually

increases, while the fluctuation of the time-varying curve of the E_0, E_6, and Z electrodes significantly weakens. This indicates that rust inhibitors and zinc-based sacrificial anodes have a certain protective effect. When the pH value decreases, the corrosion potential of the E_6 electrode has little effect, while its corrosion current density slightly weakens, indicating that the internal doped rust inhibitor has a better rust resistance effect in a neutral environment; The corrosion potential fluctuation of E_0 electrode is enhanced, and the current density slightly increases. The corrosion potential and current density are most severe at a pH value of 8.5, indicating that in a neutral environment, the migration-type rust inhibitor has poor rust resistance performance; The corrosion potential and current density of the Z electrode gradually increase, but remain within -750mV, indicating that the zinc-based sacrificial anode also has good rust resistance effect in a neutral environment.

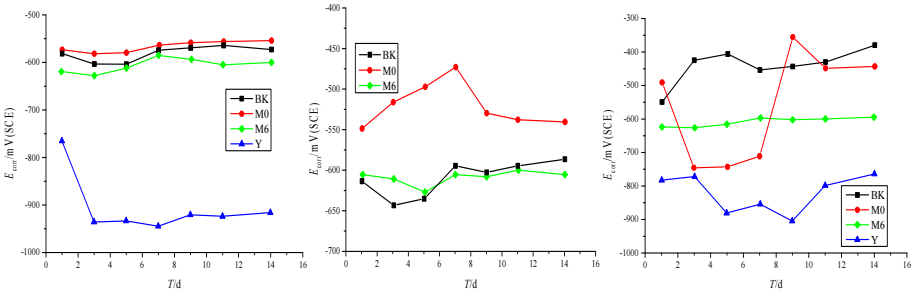

(a) C_1 (b) C_4 (c) C_3

Figure 8. Corrosion potential time-varying curve.

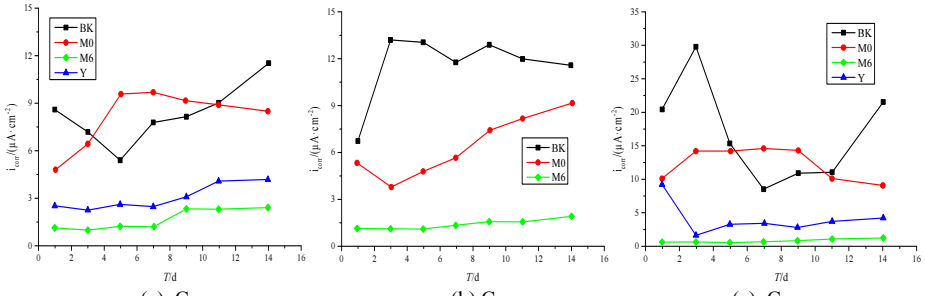

(a) C_1 (b) C_4 (c) C_3

Figure 9. Corrosion current density time-varying curve.

3.2.2. Electrochemical Impedance Spectroscopy Analysis

Figures 10 and 11 show the impedance spectra of carbon steel electrodes at different pH values, respectively. Figures 10 (a) to (c) present the Nyquist diagram of the electrode at 1d, and figures 11 (a) to (c) show the Bode phase angle diagram of the electrode at 1d. The experiment shows that the electrode capacitance arc gradually decreases with the decrease of pH value, indicating that the enhancement of acidity will accelerate the damage and corrosion rate of the passivation film on the surface of carbon steel.

To evaluate the rust resistance performance of each protective measure, equivalent circuits were selected to fit the above impedance spectra, and the protective efficiency of each protective measure was evaluated through the fitted R_{ct} values. The fitting results of some components are shown in table 3.

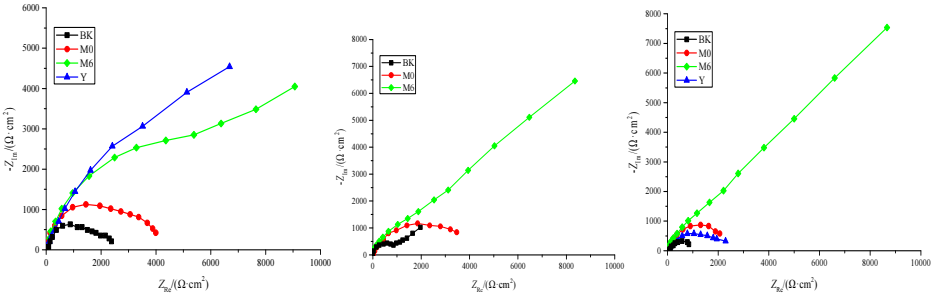

(a) C_1 (b) C_4 (c) C_3

Figure 10. Nyquist.

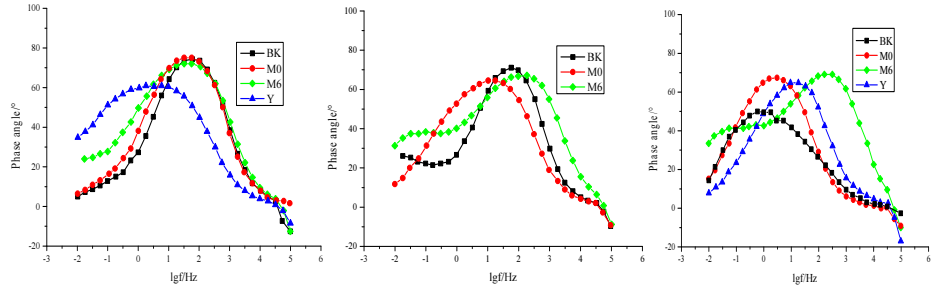

(a) C_1 (b) C_4 (c) C_3

Figure 11. Bode phase angle diagram.

Table 3 shows the protective efficiency of carbon steel electrodes under different pH environments during 1-day testing. The experimental results indicate that the protective efficiency of amino carboxylic acid type rust inhibitors increases with the decrease of pH value, with a maximum value of 98.49% at pH=8.5; The protective efficiency of migration type rust inhibitors decreases with the decrease of solution pH, with a maximum value of 61.03% at pH=12.5; the protective efficiency of zinc-based sacrificial anodes sharply decreases with the decrease of solution pH, with a maximum value of 82.05% at pH=12.5. This indicates that sacrificial anodes have good protection efficiency in alkaline environments. Therefore, when the content of rust inhibitor is 1% and the testing time is 1 day, the rust prevention performance is as follows: internal rust inhibitor>zinc-based sacrificial anode>migration type rust inhibitor (alkaline environment), internal rust inhibitor>migration type rust inhibitor>zinc-based sacrificial anode (neutral environment).

Table 3. Protective efficiency of carbon steel electrodes at different pH values.

Cases	Solution electrical protection /(Ω·cm²)	Charge transfer prevention /(Ω·cm²)	Protection efficiency /%
C_1-E_B	6.956	1369	/
C_1-E_0	7.499	3513	61.03
C_1-E_6	7.828	15280	91.04
C_1-Z	10.22	7625	82.05
C_4-E_B	8.333	1308	/
C_4-E_0	8.198	3269	59.99
C_4-E_6	9.148	34940	96.26
C_3-E_B	6.823	1249	/
C_3-E_0	8.987	2318	46.12
C_3-E_6	7.708	82550	98.49
C_3-Z	8.403	2019	38.14

3.3. Static Weightlessness Test

Table 4 lists the corrosion rate and protection efficiency of steel bars under different working conditions. From table 4, it can be known that under C_1 working conditions, the protective efficiency of the internal doping type rust inhibitor slowly decreases with time, but the migration type rust inhibitor decreases significantly. Under C_3 working conditions, the protective efficiency of migration type rust inhibitors fluctuates slightly with time, while the protective effect of zinc-based sacrificial anodes and internal doping type rust inhibitors increases slightly with time.

Table 4. Corrosion rate and protection efficiency of steel bars under different working conditions.

cases	time/d	v/(mg/(cm^2·d))	IE_w /(%)	cases	time/d	v/(mg/(cm^2·d))	IE_w /(%)
C_1-E_B	7	0.1250	/	C_3-E_B	42	0.1165	/
C_1-E_B	21	0.0493	/	C_3-E_0	7	0.0909	44.83
C_1-E_B	42	0.0303	/	C_3-E_0	21	0.0568	46.43
C_1-E_0	7	0.0568	54.55	C_3-E_0	42	0.0692	40.65
C_1-E_0	21	0.0341	30.77	C_3-E_6	7	0.0114	93.10
C_1-E_0	42	0.0246	18.75	C_3-E_6	21	0.0038	96.43
C_1-E_6	7	0.0114	90.91	C_3-E_6	42	0.0038	96.75
C_1-E_6	21	0.0057	88.46	C_3-Z	7	0.0398	75.86
C_1-E_6	42	0.0038	87.50	C_3-Z	21	0.0189	82.14
C_3-E_B	7	0.1648	/	C_3-Z	42	0.0218	81.30
C_3-E_B	21	0.1061	/				

4. Conclusions

This study investigates the protective performance of amino carboxylic acid-based internal doping, migration-type rust inhibitors, and zinc-based sacrificial anodes against steel reinforcement in concrete under varying chloride ion concentrations and pH environments. This study investigates the protective performance of amino carboxylic acid type internal doping, migration type rust inhibitors, and zinc-based sacrificial anodes against steel reinforcement in concrete under varying chloride ion concentrations and pH environments. The investigations were conducted using linear polarization, electrochemical impedance spectroscopy analysis, and static weight loss testing, leading to the following conclusions:

a) Both amino carboxylic acid type internal doping and migration type rust inhibitors can improve the concrete compactness, inhibit chloride ion penetration and carbonization (as indicated by preliminary experiments), and form a protective film on the surface of carbon steel electrodes, increasing electrode reaction impedance, and thus inhibiting steel corrosion. The internal rust inhibitor exhibits high protection efficiency but is limited to new concrete structures. The migration type rust inhibitor and zinc-based sacrificial anode protection have a wide range of applications and yield better effects in alkaline environments.
b) Across different chloride ion concentrations, the internal doping type, migration-type rust inhibitors, and zinc-based sacrificial anodes all demonstrate notable anti-corrosion effects. At the same chloride ion concentration, the internal-type rust inhibitor with the same dosage (1%) provides superior protection compared to the migration-type rust inhibitor. In environments with high chloride ion

concentrations (0.85 mol/L), zinc-based sacrificial anodes offer better protection than amino carboxylic acid rust inhibitors.

c) At different pH values under equivalent conditions, the rust resistance performance ranking in neutral environments is as follows: zinc-based sacrificial anode<migration type rust inhibitor<internal doping type rust inhibitor. In alkaline settings, the order shifts to migration-type rust inhibitors < zinc-based sacrificial anodes < internal doping-type rust inhibitors. As pH values decrease, the protective efficiency of the internal doping-type rust inhibitor increases, while the effectiveness of migration-type rust inhibitors and zinc-based sacrificial anodes decreases rapidly.

References

[1] Hou L, Ye Z, Zhou B, et al. Bond behavior of reinforcement embedded in steel fiber reinforced concrete under chloride attack. Structural Concrete. 2019; 20: 2242-2255.

[2] Sun R, Wang D, Wang Y, et al. Study on durability against dry-wet cycles and chloride ion erosion of concrete revetment materials at the water-level-fluctuations zone in yellow river delta wetlands. Wetlands. 2020; 40(6): 2713-2727.

[3] Jing L, Yin SP, Lv HL. Bonding behavior of textile reinforced concrete (TRC)-confined concrete and reinforcement under chloride erosion environment. KSCE Journal of Civil Engineering. 2020; 24(3): 826-834.

[4] Shang HS, Zhou JH, Fan GX, et al. Study on the bond behavior of steel bars embedded in concrete under the coupling of sustained loads and chloride ion erosion. Construction and Building Materials. 2021; 276: 121684.

[5] Elmoaty A. Mechanical properties and corrosion resistance of concrete modified with granite dust. Construction and Building Materials. 2013; 47: 743-752.

[6] El-Hassan, Hilal, Shehab, et al. Influence of different curing regimes on the performance and microstructure of alkali-activated slag concrete. Journal of Materials in Civil Engineering. 2018; 30(9): 04018230.

[7] Yang C, Li L, Li J. Service life of reinforced concrete seawalls suffering from chloride attack: Theoretical modelling and analysis. Construction and Building Materials. 2020; 263(4): 120172.

[8] Zhou XC, Mu S, Ma Q, et al. Accelerated evaluation of organic steel corrosion inhibitor in simulated pore solution of concrete and its equivalence analysis. Journal of the Chinese Ceramic Society. 2021; 49(8): 1713-1721.

[9] Feng X, Yan Q, X Lu, et al. Protection performance of the submerged sacrificial anode on the steel reinforcement in the conductive carbon fiber mortar column in splash zones of marine environments. Corrosion Science. 2020; 174(11): 108818.

[10] Jiang ZL, Li SY, Fu CQ, et al. Macrocell corrosion of steel in concrete under carbonation, internal chloride admixing and accelerated chloride penetration conditions. Materials. 2021; 14(24): 1-16.

[11] Jin WL, Huang N, Xu C, et al. Experimental research on effect of bidirectional electromigration rehabilitation on reinforced concrete-concentration changes of inhibitor, chloride ions and total alkalinity. Journal of Zhejiang Unviersity (Engineering Science). 2014; 48(9): 1586-1594+1609.

[12] Yan L, Song GL, Zheng D. Magnesium alloy anode as a smart corrosivity detector and intelligent sacrificial anode protector for reinforced concrete. Corrosion Science. 2019; 155: 13-28.